2014 IEEE International Conference on Robotics & Automation (ICRA)
Hong Kong Convention and Exhibition Center
May 31 - June 7, 2014. Hong Kong, China

Area of Acceptance for 3D Self-Aligning Robotic Connectors: Concepts, Metrics, and Designs

Nick Eckenstein and Mark Yim

***Abstract*— Alignment of module connectors is a crucial component of self-reconfiguration in modular robotics. Accomplishing this process using passive mechanical geometry saves resources such as space and power for the modular robot. We present concepts for evaluation of these geometries as well as a new 3D geometry, the 3D X-Face. For comparing different connectors independent of the rest of the robot, figures of merit are presented which are based on the ability for connectors to mate in the presence of position and orientation errors (offsets). Figures of merit for many current connectors are presented. The 3D X-Face alignment behavior is simulated in Gazebo over several sets of initial conditions to estimate the full area of acceptance, and the connector is tested on a CKBot robotic platform. For the situation without rotation, results indicate a 27% improvement over current gendered connectors and a 467% over ungendered connectors. The 3D X-Face is further simulated over a full five-dimensional set and metrics are estimated on that set.**

I. Introduction

Modular self-reconfigurable robot systems have been developing for several decades with many dozens of hardware systems currently proposed [1]. These systems can be categorized in to three classes based on their reconfiguration basis: lattice - where modules nominally sit on a lattice and reconfiguration occurs between neighbors, chain - where modules make and break chains, and mobile based reconfiguration - where modules move around the environment and dock independently. Docking refers to connecting and disconnecting of two modules in a given system. The docking elements of a self-reconfigurable system provide the key functionality that makes these systems self-reconfigurable.

The robustness of the docking process is often key to automatic reconfiguration. Errors in positioning and alignment for proper docking can occur from a variety of sources depending on the class of reconfiguration. Lattice-based systems tend to have the smallest amount of positional error since modules only reconfigure with neighbors. However, compliance between neighbors can lead to deformation and positional errors. Chain-based systems form arbitrarily long chains in which positional errors occur at each joint. Mobile based systems have to contend with deformations and irregularities in the environment. These errors can be compensated for either by active positioning - as would be found in chain and mobile systems, or with passive chamfer-like mechanical features which allow modules to slide into position. The latter is the main focus for this paper.

Section I introduces background and important terms. Section II explains what is meant by area of acceptance as it pertains to the examination of three-dimensional connector alignment. Section III describes a figure of merit for a self-aligning connector. Section IV reviews and compares state-of-the-art designs with the X-Face design. Section V presents details of the simulation environment used for testing. The results of the simulation and prototype testing are presented in sections VI and VII respectively.

Nick Eckenstein and Mark Yim, are from the GRASP Lab and Department of Mechanical Engineering and Applied Mechanics, at the Univ. of Pennsylvania, email: {neck,yim} @ seas.upenn.edu.

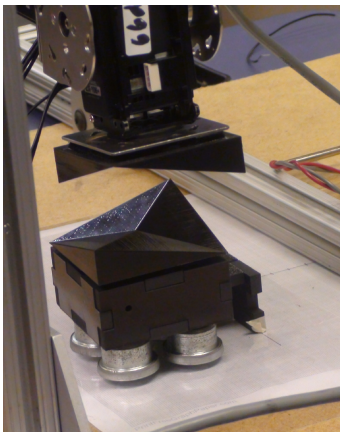

Fig. 1: Alignment test setup. Overhead arm composed of CKBots. Jig aids in setting exact position.

A. Background

We introduced the concept of **Area of Acceptance** (AA) in the previous work on the 2D X-Face. Area of acceptance is defined as 'the range of possible starting conditions for which mating will be successful' [2]. More generally, given some approach condition and pair of docking objects, the AA is the set of all initial poses (relative to each other) that result in intimate alignment of the two parts.

Few connector designs of this type have been evaluated extensively for acceptance range. Nilsson [3] mathematically determined a bound on self-alignable offsets for 2D mechanical connectors with the restriction that they be definable as a function. He applied this notion of self-alignable offsets to his characterization of the DRAGON connector [4] and determined its maximum offsets individually in all relevant degrees of freedom (DOF) ($\pm\varnothing/5$ in positional offsets [x,y], $\pm 45°$in rotational offsets [roll, pitch, yaw]). The X-Claw [5] was an active connector which had its error tolerance characterised - in (x,y,z) in combination, and (roll, pitch, yaw) individually. By utilizing multiple layers, the 2D X-Face accomplished a 200% increase in positional offset AA for 2D connectors over the bound on ungendered 2D connectors determined by Nilsson. Significant increases in combined position-orientation AA were also shown.

II. Area of Acceptance

We can classify AA into different types with respect to the DOFs of one docking element relative to the other. The DOF are either *constrained, unconstrained*, or the *approach* DOF. In the 2D X-Face, for example, the docking elements are constrained to be in a plane, and one face has three DOFs relative to the other ($SE(2)$ two of position and one of orientation). However, one of those positional DOFs include a mating direction. That DOF can be considered to be constrained while the other two are able to move freely, albeit pseudo-statically (to simplify analysis). In the more general 3D case, one face has six DOFs relative to the other ($SE(3)$) with one DOF encompassing the approach. While this approach DOF is typically considered to be a positional DOF, it could be any that lead to lower kinematic pair relationships including screws. The other five DOFs are unconstrained. Being constrained in this case means that those DOFs will always be perfectly aligned.

In some cases, where the faces have a symmetry (e.g. a round peg, in round hole) one or more DOF is in a "don't care" state. Whereas the end mating condition in all other cases has the state of all DOFs defined, this one has the other symmetric DOFs make no functional difference and so do not need to match to satisfactorily mate.

In this work, we consider the $SE(3)$ case with the approach DOF a position one which we define as the z-direction. The approach dimension is excluded from the AA as it does not affect acceptance behavior.

A. Zero Rotation Area of Acceptance

When all orientation DOF are constrained, we call the set of positions that align successfully the Zero Rotation Area of Acceptance (ZRAA). In the 2D case, this is equivalent to Nilsson's self-alignable offsets [3] as a simple bound, but in the $SE(3)$ case it represents a two-dimensional set of points (over x and y in the plane). This gives us a relatively simple, quick picture of the acceptance potential of the given connector. Some diagrams of this ZRAA are shown in Figure 2, and were determined analytically based on given dimensions of the connectors in question obtained from the literature.

System	Normalized ZRAA Sum
GENFA Connector [7]	0.00353
Polybot [8]	0.00503
M-TRAN III [9]	0.00592
JHU [10]	0.00592
I-Cubes* [11]	0.0187
CONRO* [12]	0.0425
Vacuubes [13]	0.0555
X-CLAW [5]	0.0649
ACOR(unpaired) [14]	0.0711
SINGO Connector [6]	0.306
DRAGON [4]	0.353
amour [15]	1.57
3D X-Face ^{o}	2.00

* Estimated ZRAA values.
^{o} The 3D X-Face is not a full connector. The addition of attachment capabilities will likely have some effect on the metric

TABLE I: Table of ZRAA Sum metrics, normalized relative to characteristic length of the face.

B. Full Area of Acceptance

The full AA is the AA given no exclusion of possible starting conditions and no constraints. For 2D connectors the full AA is two-dimensional (x and θ). For 3D connectors it is five-dimensional (x,y,pitch,roll,yaw). In the most general case, it is difficult to develop an analytical model to estimate AA, so empirical methods can be used. However, we have found the high dimensionality makes it costly to test or simulate exhaustively at high resolutions.

C. Other Areas of Acceptance

In order to effectively visualize the full AA without exhaustively exploring the five dimensional space, we take two dimensional slices. These slices are obtained by starting with all DOFs aligned and unconstrained, except the two being explored. Those two are sampled at high resolution to obtain an intuitive 2D plot of the AA for those DOFs.

These two dimensional subsets we call the X-Y, X-Roll, X-Pitch, and X-Yaw Areas of Acceptance (Section VI). The X-Roll Area of Acceptance is the subset of the Full AA with initial offsets in the x and roll dimensions. The others are similarly named.

III. Figure of Merit

In order to compare the ability for docking geometries to handle misalignment, we need a metric; ideally, a single figure of merit. Since connectors can be of different size, the linear dimensions are normalized to the connector size.

A. Sum Metric

The **Sum** metric is found by simply adding up the total area that is accepted. This gives a simple figure of merit of all possible configurations without giving any information as to the shape of this area. This is used in Table I, and gives a comparison for the ZRAA, where concavities are unlikely to occur and shapes are typically not complex. For example, the ZRAA for the SINGO connector, seen in Figure 2, takes up a sizeable area, but is not as robust to high error solely in x or solely in y. However, it has been our experience with the 2D X-Face that when orientation offsets are introduced irregular shapes occur. Additionally, we may find in some instances that while the sum metric for a particular connector is reasonably high, it could be highly robust to errors in one dimension, but less robust in another. In order to better measure the connector acceptance in a way that is more realistic with respect to characteristic robot error, we have developed an alternative figure of merit that reflects a range robust to errors in each dimension.

B. Oriented N-Cube Metric

Typically, each dimension has some error ranges which can be expected based on the specific robotic platform. One would like to match the positioning error with the AA. Concavities and narrow areas or holes in an AA can limit this matching. The **Oriented N-Cube Metric**, as a figure of merit is more likely able to match with errors that typically are defined as distances from an ideal position/orientation. It is defined to be a measure of the AA found by the edge size (characteristic length) of the largest axis-oriented N-Cube which fits within the normalized AA. An **N-Cube** is a

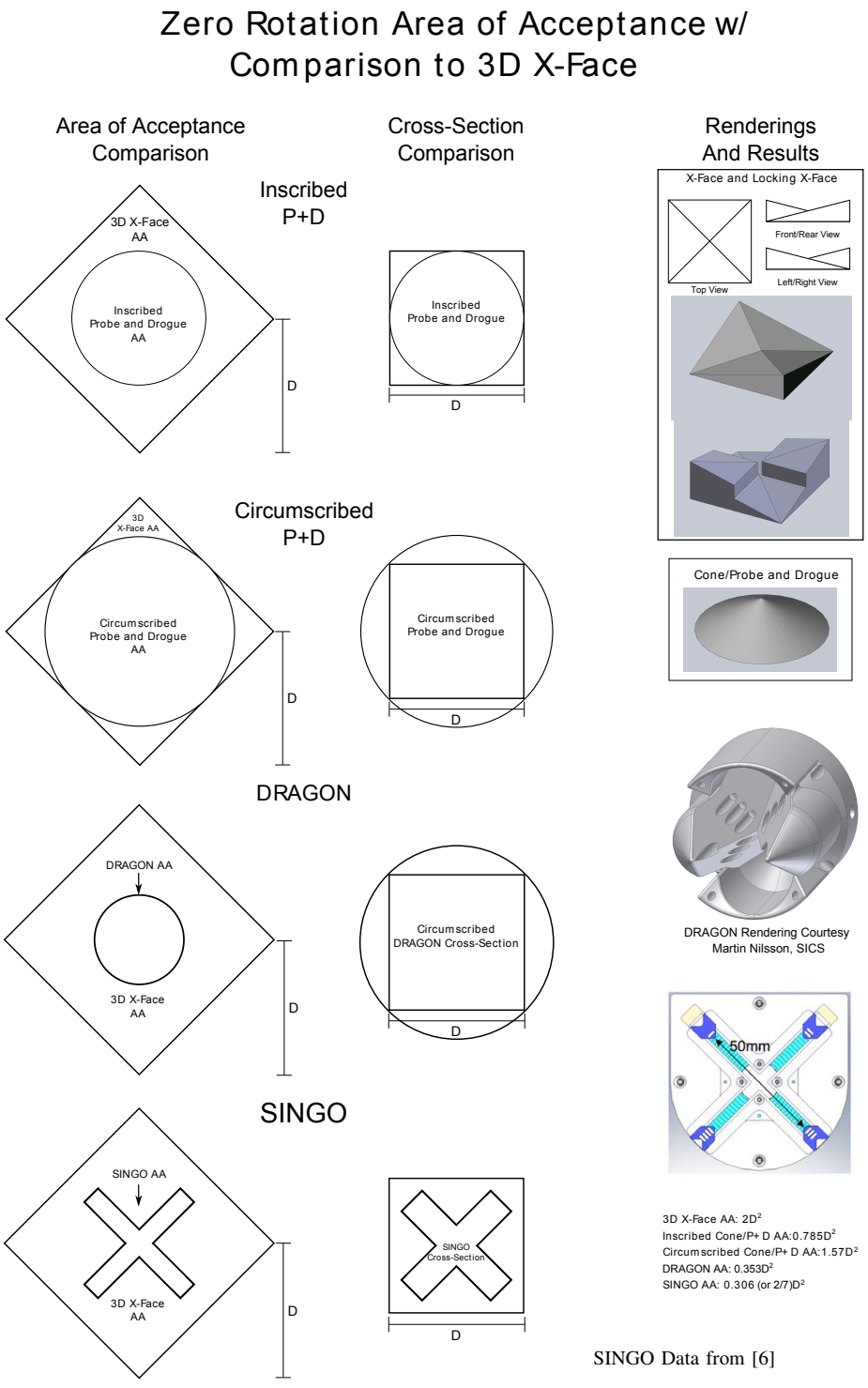

Fig. 2: Comparison of ZRAAs. The leftmost column compares ZRAAs, and the middle column compares connector cross-sections viewed from the approach direction. The large diamond shape is the ZRAA for the 3D X-Face, and other shapes correspond to the respective connectors.

cubic shape existing in N dimensions. We only consider axis-oriented *N-Cubes*, meaning that its edges are parallel to the (x,y,...) axes. For the metric we find the largest axis-oriented N-Cube which can fit fully within the normalized AA; that is, the largest N-Cube which contains only offsets that result in successful alignment. This N-Cube has a diameter (characteristic length) which is our single-number metric. The **normalized AA** is the AA with each dimension divided by its maximum feasible limits. For angular offsets this will typically be $-\pi/2$ to $\pi/2$, and for positional offsets it will be the maximum offset before connectors are no longer touching. So, on a connector with maximum positional offset of 5 mm and maximum angular offset of $\pi/2$ radians, the offset (2mm,$\pi/4$ radians) would become (0.4,0.5). Normalizing in this fashion allows us to compare angular and positional offsets and define an N-cube with unit-less measures.

The N-cube can be found mathematically; if you are sampling numerically, as we are in simulation, it is sufficient to assign each successfully docked point a number corresponding to the largest N-cube of successful points around it and take the maximum. Analytically the problem is more difficult and beyond the scope of this paper.

We can see in Fig. 2 that the largest oriented N-Cube (or square, in the case of the ZRAA) for the DRAGON or Probe and Drogue would be nearly the same area as the full sum (as the square inscribed in the circular AA), but only a small square can fit in the center of the SINGO ZRAA due to the highly concave 'X' shape.

IV. Three-Dimensional Connector Designs

In this section we detail three designs that represent the state-of-the-art with respect to self-aligning mechanical connectors and follow with a new design.

A. Existing Designs

1) Cone/Probe-and-Drogue: The first modular robot system to use a self-aligning docking connector is the cone-shaped dock on CEBOT [16], which was a simple cone-and-funnel alignment system. Other systems have used this connector shape since then, including the AMOUR underwater system [15], which called it a probe-and-drogue shape since it in fact had a 'probe' end that would be latched into the receptacle on the adjoining module. This connector is 'gendered' since it has a male face that must mate with the female face. This connector does not align offsets in the 'yaw' direction; that is, around the axis of the face.

2) Polybot: Polybot [8] used a self-aligning connector to bridge the gap over fine resolutions where sensing failed, e.g. at a chain end where errors accumulate. As a result, the 4 pin/hole pairs on each face cover a very small area compared to the face size (4mm pin diameter, 50mm face width). This connector is hermaphroditic containing both male and female parts, allowing faces to connect to any other face.

3) DRAGON Connector: Nilsson [4] was the first to use the geometry of the connector as a design feature. The DRAGON connector was designed for high-strength, high-acceptance applications, which are important for modular robotic applications as the system grows. Nilsson characterizes the offsets the connector is capable of correcting, both linear and angular (15mm=$\varnothing/5$ linearly and 45 deg angular). The DRAGON connector uses 4 cone-funnel pairs, alternating in a circle, with the latch on an outer ring.

4) Other Connectors: Other connectors have been examined, although there is not room to compare the full diagrams here. These systems are compared by ZRAA in Table I. The values in this table were determined by measurements given on the alignment geometries either in the text or in figures. Passive mechanisms are analyzed by the areas of the two aligning connector components, and active mechanisms from correction ranges given in the text.

Many modular systems are not included because they are not explicitly comparable; either the connection mechanism is not 3D, or they rely on magnetic forces to align. The systems in the table utilize either active or passive mechanical forces to align the modules for docking. Connectors utilizing active mechanisms do so as a combination alignment and attachment mechanism. Systems which use passive alignment (Cone, Polybot, DRAGON, X-Face) save a certain amount of design resources but still require latching mechanisms. Sometimes these latching mechanisms can be added with minimal effect on the area of acceptance, as in amour [15] but it still can cause constraints on the shape and dimensions.

Also worth noting are the interesting alignment geometries on many of Lipson's robots [13] [17]. These are mechanical alignment faces which augment either a pressure-driven or magnetic alignment force. When these are evaluated within the context of the paper, we evaluate only the alignment geometry, not the other forces.

B. New X-Face Designs

1) 3D X-Face: Based on on our previous geometry design, the X-Face [2], we have designed a geometry that expands the design advantages of the X-Face geometry for 3D modular robotics applications. This design was found by an attempt to find a continuous representation of the 2D X-Face; viewed from the side, we can still see that one high point is at the front-left or front-right, and the other is at the back-right or back-left respectively. Thus the 'front' and 'back' planes of the connector are geometrically similar to the two layers of the 2D X-Face as can been seen in Fig. 2.

If we think of the design as a function over a 2D plane, it appears as a function with a 'saddle' point, two minima, and two maxima. The basic geometry of the 3D X-Face connector can be seen in Figure 2. We do not have the advantage we had on the original X-Face design of an extra dimension to be utilized, but by extending the aligning faces along the full length of the sides we improve the effective AA of the connector, as we will show. This design has the advantage of being ungendered (that is, the docking faces have identical geometry), which helps with the operational flexibility of any resulting modular system by making every site eligible for docking. The design corrects for offsets in the 'yaw' direction; that is, the rotational DOF about the direction of facing. For the entirety of this paper, we use the X-Face geometry which has an angle of $\frac{\pi}{12}$, that is, $\frac{H}{D} = \sin\frac{\pi}{12}$.

We must note that the 3D X-Face is not yet a true *connector*. Without the addition of a means of physical connection it represents only an alignment geometry. Physical connections of any type require design considerations which might interfere with the ability to obtain an ideal geometry.

So while we do not consider it a precisely 'fair' comparison to other full connectors, we believe it nonetheless represents an advancement in alignment geometries over the existing literature.

We show that the 3D X-Face has ZRAA Sum of 2.0, while the next highest is the circumscribed Probe and Drogue with 1.57. This represents a 27% increase over the the best existing gendered design. The ungendered connector with the greatest ZRAA Sum is the DRAGON connector with 0.353, which we improve on by 467%. Using the Oriented N-Cube Metric, the ZRAA is measured as 1.0, equivalent to the Circumscribed Probe and Drogue. The DRAGON measured using the same metric is 0.474, so the X-Face 3D still represents an improvement of 111% for ungendered designs in this metric.

2) Locking 3D X-Face: The last design we will be comparing AA is the Locking X-Face geometry, which is a variant on the X-Face. The Locking X-Face, seen in Fig. 2, is more robust to disturbance once connected since the addition of a lip feature at the saddle point prevents the connectors from coming apart in any direction other than the facing direction. Specifically, this lip feature is the addition of a vertical (z-oriented) mating face at the center lines along each edge, meeting at the saddle point.

Twisting forces about z on the 3D X-Face without the locking feature causes the two faces to separate in the z direction. The speed of this separation is linear with the tangent of the normal of an 3D X-Face surface to z-axis (note that all four faces have the same value). In the case where the 3D X-face is flat, the tangent is 0. In this case, rotations about the z-axis yield no separation motion, yet they also yield no self-alignment behavior. When the surface normals are perpendicular to the z-axis, the tangent is infinite, and so are the separation velocities. This also corresponds to requiring infinite force (up to material strength properties). The Locking 3D X-Face exploits this principle by adding vertical faces in a lip feature.

Unfortunately the lip feature introduces the possibility of jamming due to angular misalignments or foreign material. To combat the disadvantage, the mating face of this lip feature can be given a 'draft angle' as one would in mold making. Adding a draft angle reduces the locking force from infinite, but can help prevent total failure due to dirt or other foreign object and reduce the possibility of jamming.

From a design standpoint, the locking feature also means we only have to add features to control that one DOF if we wish to ensure rigid connection once the connectors are docked successfully.

V. Simulation

A. Simulation Environment

Since we are now working in $SE(3)$, the Full AA has five dimensions . To evaluate and verify the X-Face design's AA, we utilize the Gazebo dynamic simulation environment. Gazebo was chosen because it is relatively easy to set up and repeat a simulation, and because it is capable of changing physics parameters relatively easily. This will be important for future work as we examine more of the dynamic and design space in which these connection problems occur. Gazebo also has multiple tools that can we use to ensure that the simulation's dynamic parameters (i.e. center of mass, inertia matrix) are correctly set by seeing it directly in the simulation. The default ODE physics engine was used for the simulations in this paper.

Set up of the parameters, models and environment are done by creating a standard Gazebo world file. A custom C++ plugin for Gazebo logs the results from repeating the simulation with different offsets. Alignment or failure to align was determined by measuring the distance between the 'saddle points' of the two connector models. If this distance became less than a small threshold the parts are recorded as 'aligned', but if they become too far apart (more than the width of the connector) or if the simulation runs unusually long, the parts have 'failed to align'. To ease computation, the simulation was made essentially quasi-static with large global damping. Friction and coefficient of restitution are set to zero. While not a realistic assumption, we are attempting to evaluate the alignment geometry, without choosing a material or robot. Thus it would be unfair to make any assumptions about the dynamics or material characteristics of the system. Additionally, we seek to isolate only the most basic mechanical interactions of the geometries in the scope of this experiment.

B. Simulation Parameters

The test performed to evaluate AA for the connectors in each case is a simple 'drop test'. The parts are placed over one another with initial offset and dropped under gravitational force. One part rests on a ground plane so that it does not fall away from the other part under gravity. Center of mass is placed at the connector's center of mass, so gravity forces act through that point. The gravity force is equivalent to an arm with force control on the end effector, which we will use to verify real-world acceptance with this connector.

C. Numerical Limitations

Anomalies occasionally occurred that were clearly incorrect, though this was rare (approx. 0.08%). We believe this is due to a systematic rounding error in the physics engine (ODE) that was in some cases capable of changing the outcome of a trial. However, this effect appears to be much less significant away from the boundary of the AA due to the less extreme angles involved. One set of initial conditions near the boundary was simulated approx. 12,000 times with 9 failures, while a set of initial conditions near the absolute center of the AA resulted in 0 failures after over 100,000 trials. Since the simulations sometimes consisted of upwards of 5,000 trials, occasionally this problem resulted in a disruption of the results. To combat this, we reimplemented the simulation plugin to perform each trial 3 times, with the majority result being accepted. This reduces the probability that a given data point is incorrect to 5.08×10^{-10} , but triples the computation time required.

VI. Simulation Results

A. Simulation Verification of ZRAA

A simple simulation verified the ZRAA. This was performed in Gazebo as described above. As a way to prevent rotation, the mass properties were changed. By increasing the inertia five orders of magnitude, position changes took

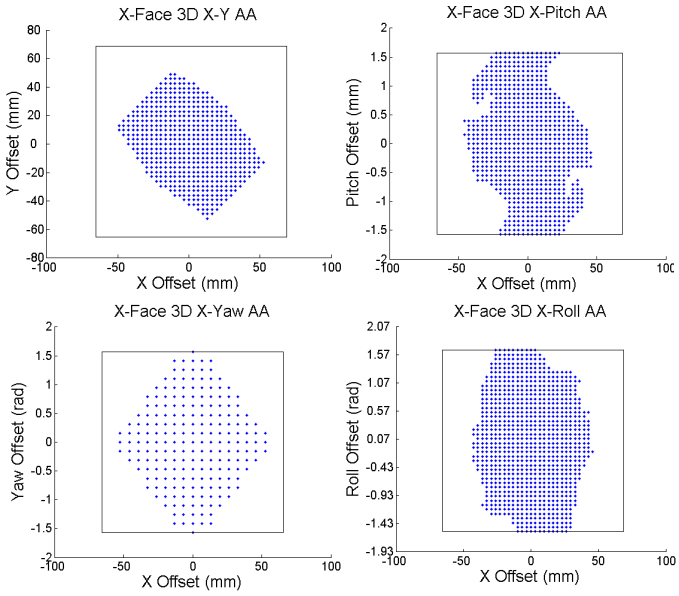

Fig. 3: Results of Simulation Testing across four selected Areas of Acceptance. Inner rectangles represent feasible range of acceptance conditions, which is the range over which acceptance was tested.

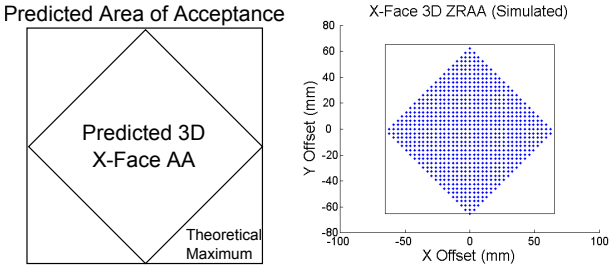

Fig. 4: ZRAA Comparison. Left: Theoretical ZRAA based on geometry. Right: Simulated ZRAA using Gazebo

extreme precedence over rotational changes. The numerical simulation results are presented side-by-side with the analytical diagram in Figure 4.

The results show a nearly perfect match between the simulation and the expected results. This verifies both that our simulator is capable of reproducing the ideal situation and that the ZRAA is as expected.

B. Simulation of Other Areas of Acceptance

The X-Y, X-Pitch, X-Roll, and X-Yaw AA an be seen in Figure 3. For these AA the inertia was returned to the correct form, but dynamic effects were reduced. To that end the gravity force was amplified (g=9000m/s^2) and added a high degree of damping. To accomplish the damping, we set the exponential velocity decay term $\alpha$for both angular and linear velocity to 0.99.

C. Discussion

While the ZRAA simulation results are straight forward, the other areas of acceptance have a more irregular shape. First, because we allow rotations in these cases, the position range is reduced, as in the X-Y AA. Second, unaligned,

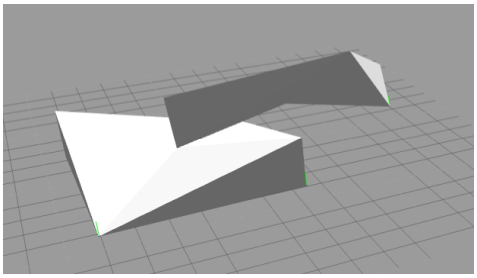

Fig. 5: A stable configuration possible when rotations are permitted. Both connectors are in contact with the ground plane.

but stable configurations arise which are the cause of the concavities visible in the other AAs. An example of a stable configuration can be seen in Figure 5. The geometry of the faces allows for a considerable range of angular offsets to be successful. Even when rotated $\frac{\pi}{2}$ in pitch or roll, the shape of the edges in conjunction with the location of the center of mass causes forcing conditions to be favorable for the connector.

Objectively, we see a relatively high acceptance for the 3D X-Face, taking up a large section of the available space. The Sum metric measurements from the simulation data for X-Y,X-Roll,X-Pitch, and X-Yaw are 0.336,0.527,0.481, and 0.504, respectively. It is difficult to accurately predict the full Sum value from these values, so we leave this to future work, when the full AA may be simulated at an acceptable resolution for analysis.

An optimistic estimate is the largest N-cube that can be formed that is consistent with the given two dimensional slices. This is found by the maximum circumscribed cube about the minimum of maximum inscribed squares of the two dimensional slice data. For orthogonal slices, this reduces to the largest n-cube which is the one with a side length equal to the length of the side of the minimum square. The Oriented N-Cube side lengths for X-Y,X-Roll,X-Pitch,and X-Yaw are 0.390,0.536,0.415,and 0.524 respectively. So the optimistic Oriented N-Cube metric is 0.390.

A more conservative estimate assumes a 'diagonal' linear relationship between 2D planes; this results in a five-dimensional 'diamond' shape. We solve this by creating a hyperplane in the positive orthant with the corner points from each of the four squares we have solved for in simulation (plus an extra point relating y and yaw; symmetry means X-Yaw is identical to Y-Yaw). We then solve for the point on that hyperplane that crosses the vector from the origin along (1,1,1,1,1). This gives us a vector (d,d,d,d,d) where d is the size of our n-cube. For the simulation data, we found this value to be 0.204.

VII. Prototype Construction and Testing

To verify our simulation results and make use of this design to dock our modular robots, prototypes of the 3D X-Face were constructed. These prototypes were constructed on the 65.5 mm x 65.5 mm scale, corresponding to the face size of the present version of CKBots [18]. The prototypes were 3D-printed on an Objet30 Photopolymer Printer out of VeroBlack material. This 3D-printing process has the

advantage of giving a smoother finish than fused-deposition modeling. The lack of friction in our prototypes aids in matching the conditions in the simulation.

The full testing setup can be seen in Figure 1. An overhead arm composed of CKBot modules carries out a vertical trajectory while the cart on casters on the bottom is free to move in the plane for alignment. Grid paper below the cart and a positioning jig let us measure the offset by hand to an estimated error range of $\pm 1mm$.

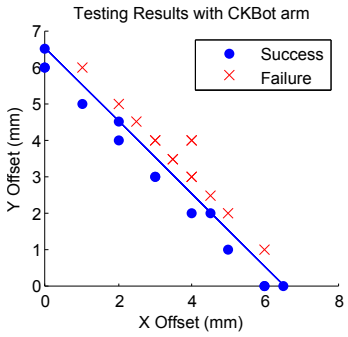

Fig. 6: Results from testing on CKBot arm platform in Fig. 1. Natural symmetry of the geometry allows us to test only a single quadrant without loss of accuracy.

Testing was carried out at select points on the boundary, in 1cm or 0.5cm increments as seen in Figure 6. No point outside the expected boundary of the AA was observed to align successfully, but instead 'rejected' the connector away. Likewise no point inside the boundary failed to align successfully, despite the proximity to the boundary of several points. This testing confirms that the ZRAA performs as expected on a real platform.

VIII. Conclusion

The 3D X-Face compares favorably to existing connectors. For ZRAA, the Sum metric was determined to be 27% larger than existing gendered connectors and 467% larger than existing ungendered connectors. The Oriented N-Cube metric showed 111% improvement over existing ungendered connectors.

The simulation results reveal stable configurations and insight into the shape of the full AA including interactions between offsets in different dimensions. From the simulation data, the estimated Oriented N-Cube metric for the full AA is 0.204 to 0.390. It is hoped that future designs can be compared with this figure of merit. Prototypes of the 3D X-Face geometry were 3D-printed and tested for ZRAA in a low-friction environment with a CKBot arm. These physical experiments validated the simulation and analysis.

In future work, we will examine design parameters like aspect ratio (connector height compared to cross-section), center of rotation, and kinematic restrictions. Dynamic interactions should be explored. Varying the approach path has a significant effect on the acceptance, and many self-reconfigurable systems do not have a perpendicular approach. In the future we may replace the faces of the CKBots with a latching version of this connector for full reconfigurability. This would allow us to gain the advantages of the 3D X-Face alignment without changing the connectability of the system. A latch on the exterior of the face similar to the DRAGON connector, could possibly add latching with minimal effect on the alignment geometry.

Acknowledgements: The authors would like to thank Martin Nilsson, SICS for his essential information on the DRAGON Connector.

References

[1] K. Støy, *An Introduction to Self-Reconfigurable Robots*. Boston, MA: MIT Press, 2009.

[2] N. Eckenstein and M. Yim, "The x-face: An improved planar passive mechanical connector for modular self-reconfigurable robots," in *IEEE/RSJ International Conference on Intelligent Robots and Systems (IROS)*. IEEE, 2012, pp. 3073–3078.

[3] M. Nilsson, "Symmetric docking in 2d: A bound on self-alignable offsets," in *IASTED '99: Robotics and Automation*, Oct. 1999.

[4] ——, "Connectors for self-reconfiguring robots," *IEEE/ASME Transactions on Mechatronics*, vol. 7, no. 4, pp. 473–474, 2002.

[5] J. J. Cong and R. Fitch, "The x-claw self-aligning connector for self-reconfiguring modular robots," in *IROS '11: Proceedings of the Workshop on Reconfigurable Modular Robotics: Challenges of Mechatronic and Bio-Chemo-Hybrid Systems*, 2011.

[6] W.-M. Shen, R. Kovac, and M. Rubenstein, "Singo: A single-end-operative and genderless connector for self-reconfiguration, self-assembly and self-healing," in *IEEE International Conference on Robotics and Automation*, 2009, pp. 4253–4258.

[7] G. Fu, A. Menciassi, and P. Dario, "Development of a genderless and fail-safe connection system for autonomous modular robots," in *IEEE International Conference on Robotics and Biomimetics (ROBIO)*, 2011, pp. 877–882.

[8] M. Yim, D. Duff, and K. Roufas, "Polybot: a modular reconfigurable robot," in *Proceedings. ICRA '00. IEEE International Conference on Robotics and Automation*, vol. 1, 2000, pp. 514–520 vol.1.

[9] H. Kurokawa, K. Tomita, A. Kamimura, S. Kokaji, T. Hasuo, and S. Murata, "Distributed self-reconfiguration of m-tran iii modular robotic system," *The International Journal of Robotics Research*, vol. 27, no. 3-4, pp. 373–386, 2008. [Online]. Available: http://ijr.sagepub.com/content/27/3-4/373.abstract

[10] M. Kutzer, M. Moses, C. Brown, D. Scheidt, G. Chirikjian, and M. Armand, "Design of a new independently-mobile reconfigurable modular robot," in *IEEE International Conference on Robotics and Automation (ICRA)*, 2010, pp. 2758–2764.

[11] C. Unsal and P. K. Khosla, "Solutions for 3d self-reconfiguration in a modular robotic system: implementation and motion planning," vol. 4196, 2000, pp. 388–401. [Online]. Available: http://dx.doi.org/10.1117/12.403737

[12] A. Castano, A. Behar, and P. Will, "The conro modules for reconfigurable robots," *IEEE/ASME Transactions on Mechatronics*, vol. 7, no. 4, pp. 403–409, 2002.

[13] R. Garcia, J. Hiller, K. Stoy, and H. Lipson, "A vacuum-based bonding mechanism for modular robotics," *IEEE Transactions on Robotics*, vol. 27, no. 5, pp. 876–890, 2011.

[14] M. Badescu and C. Mavroidis, "Novel active connector for modular robotic systems," *IEEE/ASME Transactions on Mechatronics*, vol. 8, no. 3, pp. 342–351, 2003.

[15] I. Vasilescu, P. Varshavskaya, K. Kotay, and D. Rus, "Autonomous modular optical underwater robot (amour) design, prototype and feasibility study," in *Proceedings of the 2005 IEEE International Conference on Robotics and Automation*, april 2005, pp. 1603 – 1609.

[16] T. Fukuda, M. Buss, H. Hosokai, and Y. Kawauchi, "Cell structured robotic system cebot: Control, planning and communication methods," *Robotics and Autonomous Systems*, vol. 7, no. 23, pp. 239 – 248, 1991, special Issue Intelligent Autonomous Systems. [Online]. Available: http://www.sciencedirect.com/science/article/pii/092188909190045M

[17] G. Studer and H. Lipson, "Spontaneous emergence of self-replicating structures in molecube automata," in *Proc. of the 10th Int. Conf. on the Simulation and Synthesis of Living Systems (Artificial Life X)*, 2006, pp. 227–233.

[18] J. Davey, J. Sastra, M. Piccoli, and M. Yim, "Modlock: A manual connector for reconfigurable modular robots," in *IEEE/RSJ International Conference on Intelligent Robots and Systems (IROS)*, 2012, pp. 3217–3222.